

## Influence of the Vertical Track Irregularities upon the Wheel-Rail Dynamic Forces

Mădălina Dumitriu\* and Ioan Sebeșan

Department of Railway Vehicles, Faculty of Transport, University Politehnica of Bucharest, 313 Splaiul Independenței, 060042, Bucharest, Romania

Received 8 October 2016; Accepted 18 January 2017

### Abstract

This paper is focused on the study of the wheel-rail dynamic force caused by the interaction between a moving wheel and a rail with vertical irregularities. Three cases have been considered: (a) track with random irregularities, (b) track with joints and (c) track with isolated error. The results demonstrate that the magnitude of the dynamic forces is dependent on the velocity, track quality and, also, on the characteristics of the track irregularities and on the track damping

*Keywords:* wheelset, dynamic force, vertical track irregularities, joint, isolated track error

### 1. Introduction

While rail vehicles are running over the irregularities of the rolling track of the rails [1], over their discontinuities (joints, switch points, crossings) [2], or when one of the vehicle wheels is rolling over a local error of its own rolling surface (eg. the flat rolling surface) [3], dynamic contact overlapping static forces occur at the wheel-rail interface.

As a function of their size, the dynamic forces can develop an important level of stress in the running gear and the track, which affects both the wheel endurance and of the other components of the running gear and of the rail's [4 - 6].

It is worthy mentioning a wear and tear condition on the rolling surface of the wheels and rails' [7], along with the generation of the rolling noise [8, 9]. It is well known that one of the railway vehicle homologation criterion (track fatigue stress) requires the upper limits for wheel-rail dynamic force [10, 11].

This paper presents the influence of the vertical track irregularities on the wheel-rail dynamic force considering three track irregularity types.

Firstly, there will be an analysis of the track quality influence, in correlation with its velocity and damping degree, upon the frequency response functions of the dynamic forces while having the wheelset run over a track with random irregularities, introduced by the numerical model as stochastic data defined by the power spectral density (PSD) [12]. Secondly, the wheel/rail dynamic force is calculated when the wheel runs along a track with joints aiming to show how the magnitude of the track irregularity becomes an impact factor on the contact force between wheel and rail at different speeds. Lastly, the attention is paid on the track damping impact on the peaks of the contact force caused by the wheel running along a track with

isolated error.

### 2. The Mechanical Model To Study The Wheelset Vertical Vibrations

To study the wheelset vibrations derived from the vertical track irregularities, the mechanical model in Fig. 1 [13, 21] is considered. It is about an oscillating system comprised of the wheelset of mass  $m_w$  and the track reduced mass  $m_t$ . The following track parameters are also considered:  $k_t$  – track rigidity and  $c_t$  – track damping coefficient.

The wheelset runs at the speed  $V$  over a track vertical irregularity defined by the variable depth  $\eta$  (due to the static load effect). The acceleration conveyed to the wheelset using the rolling over the track irregularity will make emerge an inertia force that manifests as a dynamic contact force whose action will trigger an additional track bending (of a dynamic nature)  $\Delta\eta$ .

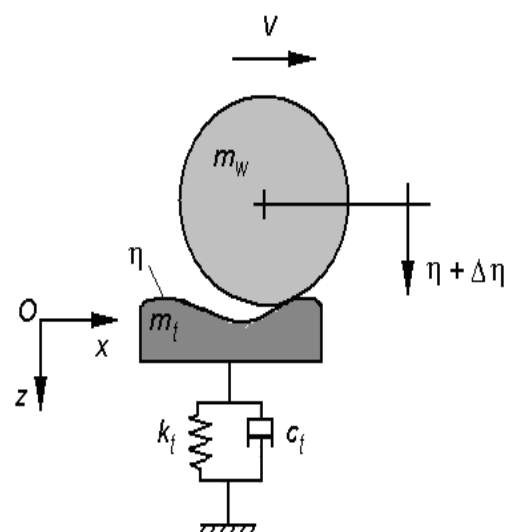


Fig. 1. The mechanical model of the wheelset/track system [13, 21].

The equation of motion for the wheelset writes as

$$(m_w + m_t) \frac{d^2(\eta + \Delta\eta)}{dt^2} + c_t \frac{d\Delta\eta}{dt} + k_t \Delta\eta = 0. \quad (1)$$

Should the notation  $z = \eta + \Delta\eta$  is introduced and the track reduced mass compared to the wheelset's is overlooked, the Eq. (1) will be

$$m_w \ddot{z} + c_t (\dot{z} - \dot{\eta}) + k_t (z - \eta) = 0, \quad (2)$$

or

$$m_w \ddot{z} + c_t \dot{z} + k_t z = c_t \dot{\eta} + k_t \eta \quad (3)$$

The wheelset equation of motion will be used in the following sections for calculating the frequency response functions of the dynamic forces in a permanent harmonic regime of vibration and for the dynamic forces during the rolling on a track with joints or crossing an isolated track error.

### 3. Mathematical Model of the Track Irregularities

The track geometry irregularities represent the primary inputs in the numerical simulations for the dynamics of the railway vehicles. The track irregularities can be represented following two distinct methods [14]. One method considers the irregularities of the track as functions of distance along the track (modelling in space domain) [14-16]. Another one takes into account the random character of the track irregularities as stationary stochastic process and uses the power spectral density to represent them in the frequency domain [17-19].

### 4. The Track Irregularities Modelling in the Frequency Domain

In Europe, the frequency domain representation of the track irregularities starts from the bellow form in terms of the power spectral density in the space domain [20]

$$S(\Omega) = \frac{A\Omega_c^2}{(\Omega^2 + \Omega_c^2)(\Omega^2 + \Omega_r^2)} \quad (4)$$

where  $W$  is the wavenumber ( $W = 2\pi/\Lambda$ , where  $L$  is the wavelength),  $A$  is coefficient depending on the track quality, and  $\Omega_c$  and  $\Omega_r$  are values which are derived from experiments in terms of wavenumbers. For instance,  $A = 4.032 \cdot 10^{-7}$  radm corresponds to high level quality, while  $A = 1,080 \cdot 10^{-6}$  radm corresponds to low level quality. The coefficients  $\Omega_c$  and  $\Omega_r$  have the following values:  $\Omega_c = 0.8246$  rad/m and  $\Omega_r = 0.0206$  rad/m.

To obtain the representation of the PSD track irregularities in the frequency domain, the general equation is utilised

$$G(\omega) = \frac{S(\omega/V)}{V}, \quad (5)$$

where  $\omega = V\Omega$  is the angular frequency which corresponds to the wavenumber  $W$  at the speed  $V$ .

Finally, it obtains the frequency domain representation of the PSD track irregularities

$$G(\omega) = \frac{A\Omega_c^2 V^3}{[\omega^2 + (V\Omega_c)^2][\omega^2 + (V\Omega_r)^2]}. \quad (6)$$

### 4.1 Modelling Of The Track With Joints

According to the fig. 2, the track with joints can be represented using the following form [13, 21]

$$\eta = \frac{H_0}{2} \left( 1 - \cos \frac{2\pi x}{L_0} \right) \text{ for } 0 \leq x \leq L_0 \quad (7)$$

where  $H_0$  is the magnitude of the track irregularity due to the joint (medium magnitude is  $H_0 = 1$  cm) and  $L_0$  is the joint length which varies from 1 to 5 meters (average  $L_0 = 2.5$  m).

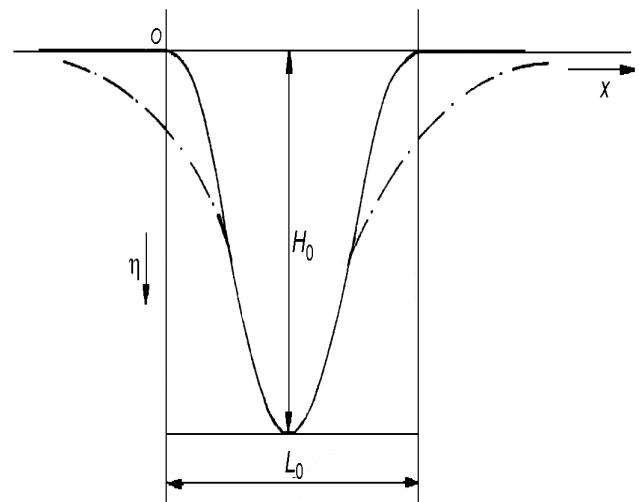


Fig. 2. Mathematical modelling of the joint profile: - - -, real profile of joint; —, theoretical joint profile (see Eq. (7)).

However, the track with joints, like one with continuous welded rails, has also vertical irregularities which appear during the construction, exploitation or as effect of slow motion of the soil or other environment factors [14].

The sinusoidal form is simplest way to represent the above vertical irregularities of the track. For instance, considering the fixed length of the rail,  $L$ , and amplitude of the irregularities,  $H_1$ , it can write

$$\eta_t = H_1 \cos \frac{4\pi x}{L} \quad (8)$$

where  $x$  is the coordinate along the track and  $H_1$  can take values between  $0.25H_0$  and  $0.5H_0$  with an average value of  $0.35H_0$ .

The vertical motion of the axle can be described by the following equation

$$\eta_w = \eta_t = H_1 \cos 2\omega t. \quad (9)$$

where  $\omega = 2\pi V/L$  is half angular frequency of the vertical motion of the axle which runs at  $V$  speed along the track.

Moving on a track with joints, the vehicle experiences both periodic and aperiodic motion due to the axle perturbation motion coming from the sinusoidal

irregularities and joints, respectively. This is the case when the shock occurred by the joints is attenuated along the distance between two successively joints. Alternatively, the joints induce a periodic perturbation of  $w$  angular frequency.

For this situation, the track registered profile can be roughly substituted with a curve (Fig. 3), with the equation

$$\eta = \frac{H_0}{2} \left( 1 - \cos \frac{2\pi x}{L} \right) + H_1 \cos \frac{4\pi x}{L}, \quad (10)$$

and the axles will generate a disturbance as in the function below

$$\eta = \frac{H_0}{2} (1 - \cos \omega t) + H_1 \cos 2\omega t. \quad (11)$$

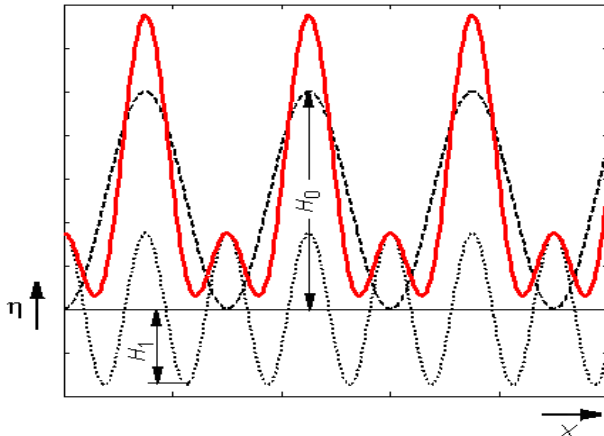


Fig. 3. Idealised profile of the tracks with joints: —,  $\eta$ ; - - -,  $\eta_j$ ; .....  $\eta_i$ ;

Fig. 3 shows the idealised profile of the track with joints according to the Eq. (10), and its components: the joint profile ( $\eta_j$ ), and the irregularities profile, respectively ( $\eta_i$ ) [22]

$$\eta_j = \frac{H_0}{2} \left( 1 - \cos \frac{2\pi x}{L} \right); \quad \eta_i = H_1 \cos \frac{4\pi x}{L}. \quad (12)$$

### 5. The Wheelset Frequency Response Functions

Both the vertical track irregularities and the wheelset response are considered to be harmonic functions in the below form

$$\eta = \eta_0 \cos \omega t; \quad z = z_0 \cos(\omega t + \alpha), \quad (13)$$

where  $\omega = 2\pi v$  is the pulsation of the excitation corresponding to frequency  $v$ , due to the wheel crossing over the track irregularities at speed  $V$ ,  $\eta_0$  excitation amplitude,  $z_0$  – amplitude of the wheelset displacement, and  $\alpha$  the phase difference between the wheelset displacement and excitation  $\eta$ .

When the complex units associated with real ones are introduced, the functions  $\eta$  and  $z$  are written as such

$$\bar{\eta} = \bar{\eta}_0 e^{i\omega t}; \quad \bar{z} = \bar{z}_0 e^{i(\omega t + \alpha)}, \quad \text{with } i^2 = -1. \quad (14)$$

When the relations (14) are further introduced in the differential equation of motion (3), an algebraic equation is derived

$$(-m_w \omega^2 + i c_t \omega + k_t) \bar{z}_0 = (i c_t \omega + k_t) \bar{\eta}_0, \quad (15)$$

from which the response function of the wheelset vertical displacement results

$$\bar{H}_z(\omega) = \frac{\bar{z}_0}{\bar{\eta}_0} = \frac{i c_t \omega + k_t}{-m_w \omega^2 + i c_t \omega + k_t}. \quad (16)$$

$$\text{If } \omega_t = \sqrt{k_t / m_w} \quad (17)$$

notes the natural pulsation of the wheelset-track vibrant system and

$$\zeta_t = \frac{c_t}{2\sqrt{k_t m_w}}, \quad (18)$$

is the track damping degree, then the response function of the wheelset vertical displacement can be calculated with the relation

$$H_z = |\bar{H}_z| = \frac{|2i\omega\omega_t\zeta_t + \omega_t^2|}{|\omega_t^2 - \omega^2 + 2i\omega\omega_t\zeta_t|} = \frac{\sqrt{\omega_t^4 + 4\omega^2\omega_t^2\zeta_t^2}}{\sqrt{(\omega_t^2 - \omega^2)^2 + 4\omega^2\omega_t^2\zeta_t^2}}. \quad (19)$$

Further on, the expression of the response function can be written

$$H_z(\omega) = \sqrt{\frac{1 + 4\zeta_t^2(\omega / \omega_t)^2}{[1 - (\omega / \omega_t)^2]^2 + 4\zeta_t^2(\omega / \omega_t)^2}}. \quad (20)$$

Based on the response function  $H_z$  of the wheelset vertical displacement, the response function of its acceleration  $\ddot{z}$  will be calculated,

$$H_{\ddot{z}}(\omega) = \omega^2 H_z(\omega). \quad (21)$$

The wheelset vertical vibrations will generate dynamic forces, noted with  $\Delta q$ , on the wheels and trails contact. The response function of the dynamic forces is in the relation:

$$H_{\Delta q} = m_w H_{\ddot{z}}(\omega) = m_w \omega^2 H_z(\omega). \quad (22)$$

The frequency response functions that are specific to the permanent harmonic vibration regime underlie the calculation of the frequency response functions pertinent to the random regime of vibrations, as seen hereafter.

Using Eqs. (6) and (22), the PSD of the dynamic forces results as

$$G_{\Delta q}(\omega) = G(\omega) H_{\Delta q}^2(\omega) = m_w^2 \omega^4 H_z^2(\omega). \quad (23)$$

If replacing the relations corresponding to  $H_z^2(\omega)$  and  $G(\omega)$ , the Eq. (23) becomes

$$G_{\Delta q}(\omega) = m_w^2 \frac{A\Omega_r^2 V^3}{[\omega^2 + (V\Omega_r)^2][\omega^2 + (V\Omega_r)^2]} \cdot \frac{1 + 4\zeta_r^2(\omega/\omega_r)^2}{[1 - (\omega/\omega_r)^2]^2 + 4\zeta_r^2(\omega/\omega_r)^2} \quad (24)$$

Finally, the mean square deviation of the dynamic forces is obtained

$$\sigma_{\Delta q} = \sqrt{\frac{1}{\pi} \int_0^{\infty} G_{\Delta q}(\omega) d\omega} \quad (25)$$

considering the angular frequency corresponding to 100 Hz the upper limit under integral, according to the validity domain of the model.

### 6. Numerical Application

Next, the numerical results derived from the above model are presented considering a wheelset running on a track with: (a) random irregularities; (b) joints; and (c) isolated error. Corresponding to these three cases, the section goals consist of the examination of the follow aspects: (a) the impact of the track quality on the dynamic force in connection to the two important parameters, namely, the wheel velocity and damping of the track; (b) the influence of the irregularities amplitude on the wheel/rail dynamic force; (c) the influence of the track damping upon the dynamic force between wheel and rail.

The Fig. 4 shows the response function of the dynamic forces during the rolling of a wheelset on a track with vertical irregularities in a harmonic form. The following parameters of numerical simulation have been taken into account: wheelset mass  $m_w = 2000$  kg, track stiffness  $k_t = 10^8$  N/m, and for the track damping degree ( $z_t$ ) values within the interval of 0.1 ... 0.3 have been adopted. The dynamic force reaches its maximum value at the resonance frequency of the wheel/track system (circa 33 Hz). The track damping degree will be also visible at this frequency. A higher  $z_c$  will lead to a weaker response function of the dynamic forces. The track damping impact on the dynamic force is small at sub-critical frequencies and high at over-critical frequencies.

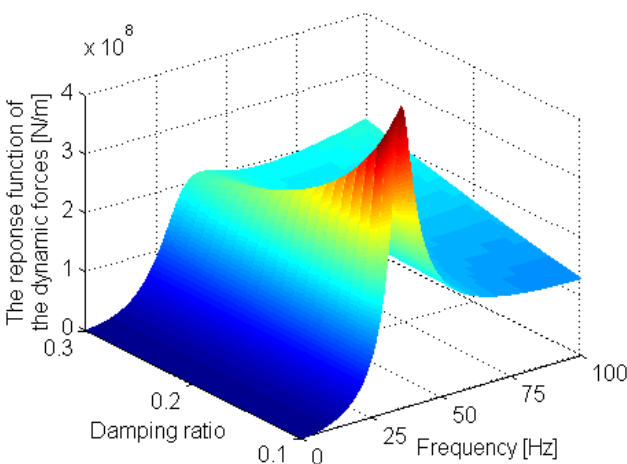


Fig. 4. The response function of the dynamic forces.

Given that the wheelset is rolling on a track with random vertical irregularities, described via the PSD according to

Eq. 6, the PSD for the dynamic forces at velocities up to 200 km/h has been calculated for both a high level quality track defined by constant  $A = 4.032 \cdot 10^{-7}$  radm (see Fig. 5), and a low level quality track with the constant  $A = 1.080 \cdot 10^{-6}$  radm (see fig. 6). Three values of the track damping degree have been considered, namely  $z_t = 0.1$  (diagrams (a));  $z_t = 0.2$  (diagrams (b));  $z_t = 0.3$  (diagrams (c)).

It can observe that the PSD of the dynamic forces preserves the main features of the response function, i.e. it reaches its maximum values at the resonance frequency of the wheel/track system and it increases along the wheel velocity.

Next, the track damping impact upon the PSD dynamic force is examined. This is visible in both the diagrams in Fig. 5 and in Fig. 6, where the decrease of the peak of the spectral density corresponding to the wheelset resonance frequency is evident with the increase of the track damping degree. The Table 1 includes the maximum values of  $G_{\Delta q}$  calculated for the rolling of wheelset at velocity of 200 km/h on a high level quality track and on a low level quality track. An increase in the track damping from 0.1 to 0.2 has as effect the decrease of PSD dynamic forces between 68% and 83%, if  $z_t$  increases between 0.1 and 0.3.

Table 1. The PSD of the dynamic forces at the resonance frequency of the wheel/track system at 200 km/h.

Damping ratio of the track	$z_t = 0.1$	$z_t = 0.2$	$z_t = 0.3$
Track quality	PSD of the dynamic forces [kN <sup>2</sup> /Hz]		
$A = 4.032 \cdot 10^{-7}$ radm	4.22	1.34	0.71
$A = 1.080 \cdot 10^{-6}$ radm	11.31	3.59	1.90

Also based on the diagrams in Fig. 5 and Fig. 6, the track quality impact on the PSD dynamic forces can be analysed. If the maximum values of  $G_{\Delta q}$  at 200 km/h velocity for the wheelset resonance frequency are considered for comparison (see Table 1), the conclusion is that, irrespective of the track damping degree, these values are circa 2.7 higher for a wheelset rolling over a low level quality track ( $A = 1.080 \cdot 10^{-6}$  radm) than for the same action on a high level quality track ( $A = 4.032 \cdot 10^{-7}$  radm).

Figure 7 shows the root mean square (RMS) of the dynamic forces calculated as a function of velocity and track damping degree. An approximately linear increase of the dynamic forces is evident, depending on velocity; also, the higher the growth rate, the lower the damping on the track. For instance, while the wheelset is running on a high level quality track (diagram (a)) at velocity of 200 km/h, the result is  $\sigma_{\Delta q} = 1.4$  kN for  $z_t = 0.1$ , whereas a track damping degree of  $z_t = 0.3$  will derive a value of 0.98 kN. Similar differences will be obtained when the wheelset is running over a low level quality track (diagram (b)), namely  $\sigma_{\Delta q} = 2.3$  kN for  $z_t = 0.1$  and  $\sigma_{\Delta q} = 1.6$  kN for  $z_t = 0.3$ .

The above-mentioned values also prove the influence of the track quality upon the size of the dynamic forces. For a wheelset running on a low level quality track, these forces are circa 38% higher than for a high level quality track.

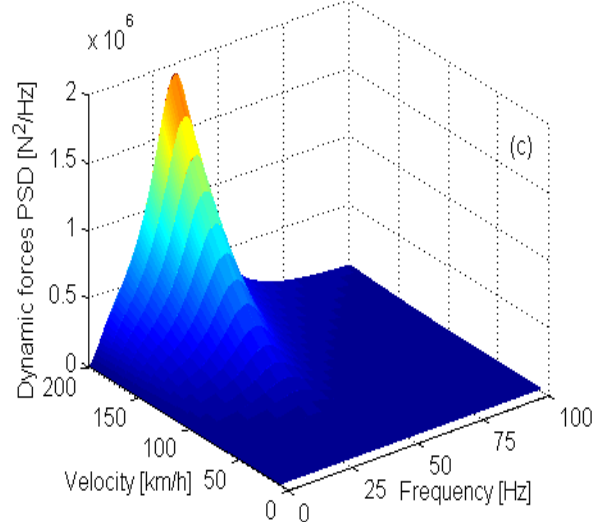
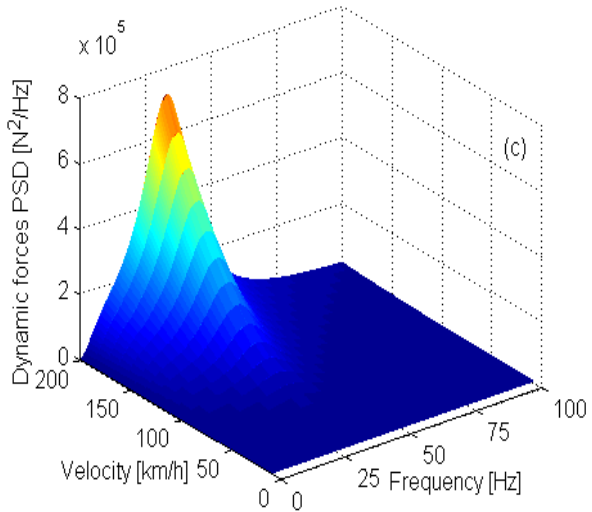
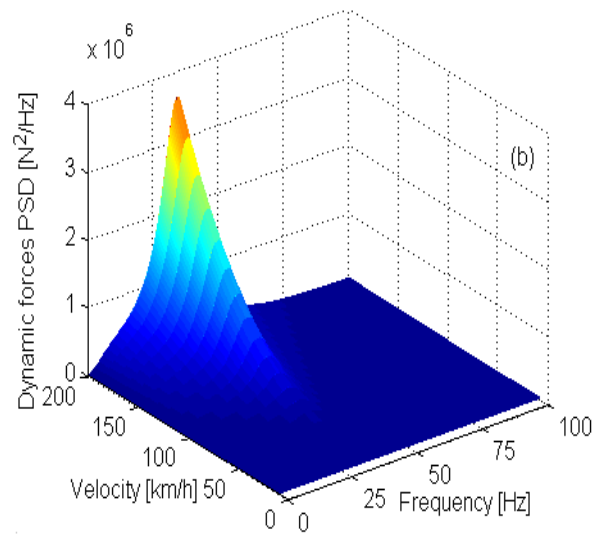
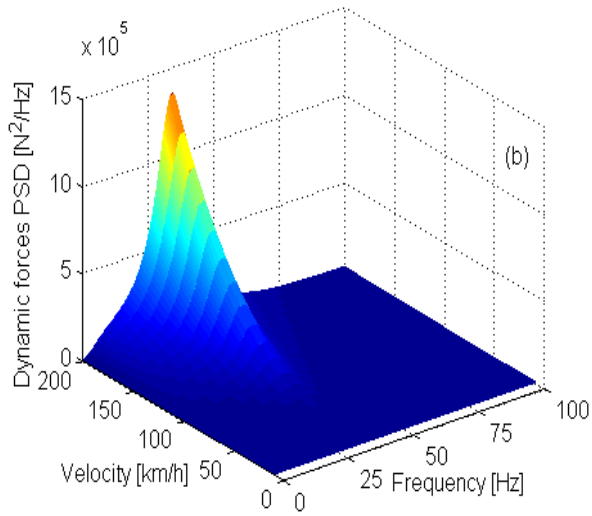
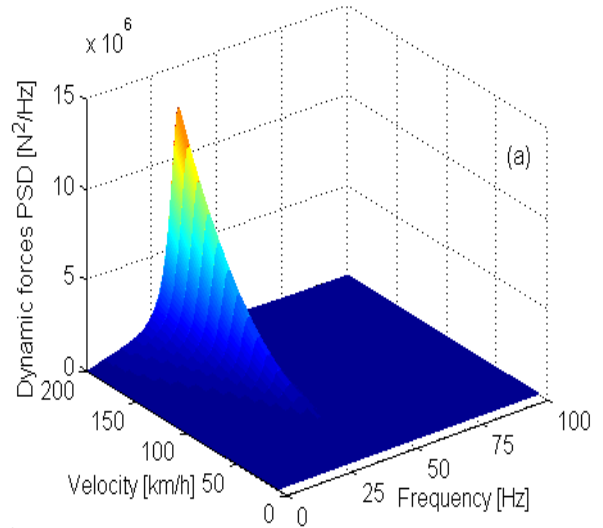
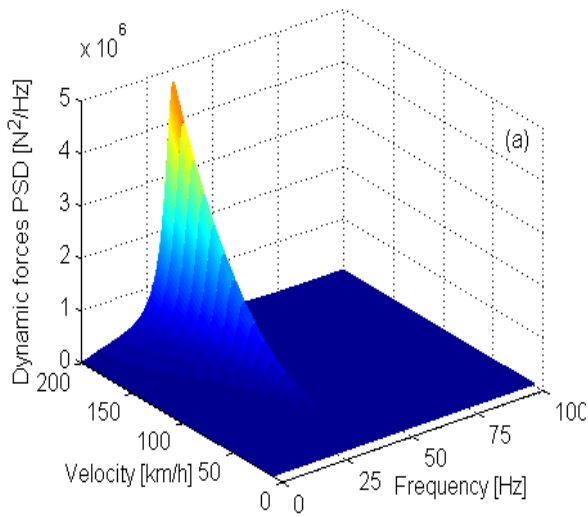


Fig. 5. PSD of the dynamic forces on a high level quality track: (a)  $z_c = 0.1$ ; (b)  $z_c = 0.2$ ; (c)  $z_c = 0.3$ .

Fig. 6. PSD of the dynamic forces on a low level quality track: (a)  $z_c = 0.1$ ; (b)  $z_c = 0.2$ ; (c)  $z_c = 0.3$ .

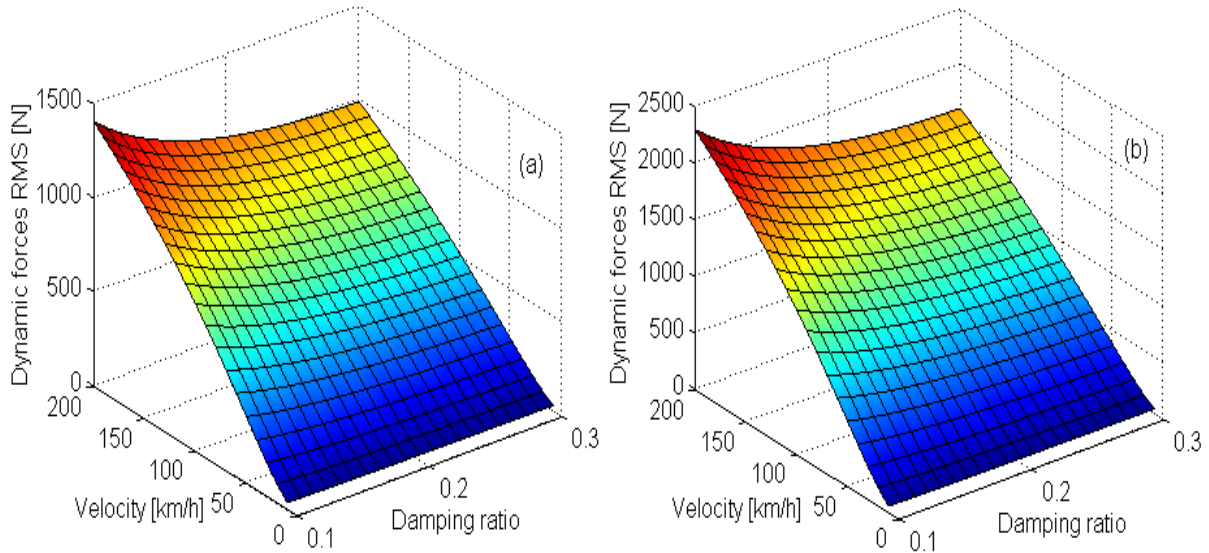


Fig. 7. The root mean square of the dynamic forces: (a) high level quality track ( $A = 4.032 \cdot 10^{-7}$  radm); (b) low level quality track ( $A = 1.080 \cdot 10^{-6}$  radm).

Fig. 8 features the dynamic forces calculated for the velocities of 40 km/h, 80 km/h and 120 km/h recorded for a wheelset rolling over a track with joints. The following parameters for the track irregularities have been considered:  $L = 15$  m,  $H_1 = 0.35H_0$  and  $H_0 = 0.01$  m. It hence becomes obvious that the dynamic forces increase with the velocity:  $\Delta q = 0.61$  kN for  $V = 40$  km/h;  $\Delta q = 2.48$  kN for  $V = 80$  km/h and  $\Delta q = 5.63$  kN for  $V = 120$  km/h.

Fig. 9 highlights the rise of the dynamic forces along with the amplitude in the track geometric irregularities on a rail with joints, for the velocities of 40 km/h, 80 km/h and 120 km/h. In other words, for an increase of  $H_1$  from  $0.25H_0$  to  $0.35H_0$ , the dynamic forces will go upwards by circa 27%, whereas for a  $H_1$  from  $0.25H_0$  to  $0.45H_0$ , the percentage will be circa 43%.

Further on, the time-based evolution of the size of dynamic forces will be examined, when the wheelset is crossing an isolated track error, described by

$$\eta = \eta_0 \sin^2 \frac{\pi x}{L}, \quad 0 \leq x \leq L; \tag{26}$$

$$\eta = 0, \quad x > L,$$

where  $\eta_0$  is the error amplitude and  $L$  its length [21].

For the numerical simulations, the following parameters of the isolated error have been considered:  $\eta_0 = 9$  mm;  $L = 9$  m. Similarly, to calculate the dynamic forces while running over the isolated error, the velocities of 100 km/h (Fig. 10) and 200 km/h (Fig. 11) have been viewed, while for the track damping degree, we have the values  $z_t = 0.1$  (diagrams (a));  $z_t = 0.2$  (diagrams (b));  $z_t = 0.3$  (diagrams (c)). The positive values of the dynamic forces show the download of the wheel-rail contact whereas the negative ones are for a contact upload.

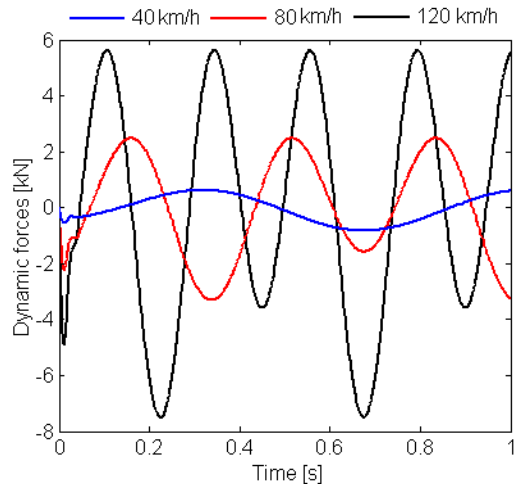


Fig. 8. Influence of the velocity upon the dynamic forces.

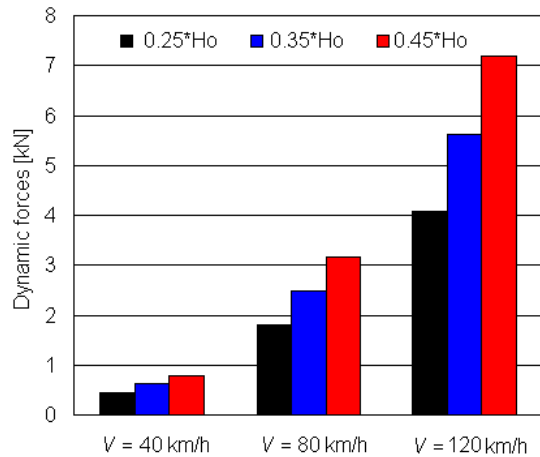
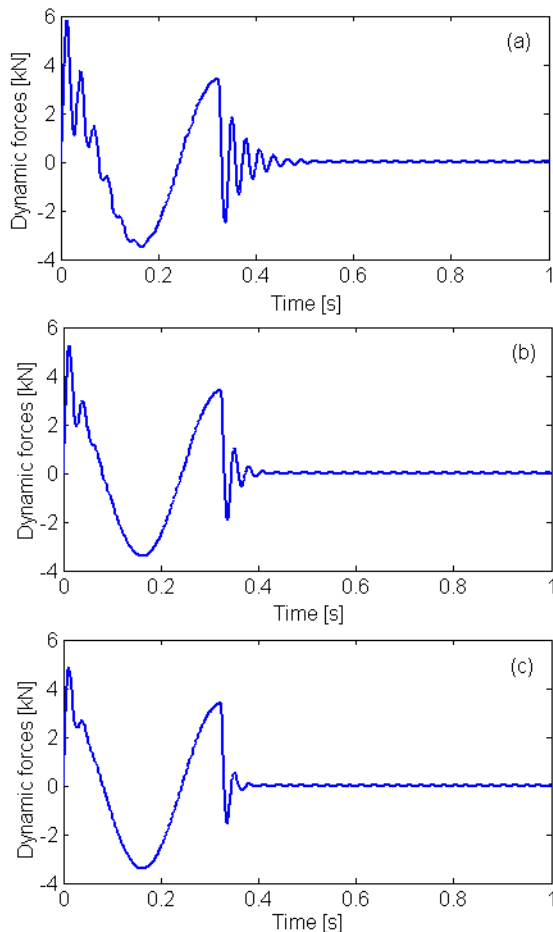


Fig. 9. Dynamic force versus amplitude of the track irregularities.



**Fig. 10.** Dynamic forces when crossing over the isolated error at velocity of 100 km/h: (a)  $z_t = 0.1$ ; (b)  $z_t = 0.2$ ; (c)  $z_t = 0.3$ .

In the first part of the numerical simulation, the contact force decreases due to mix effect of the wheel inertia and isolated error shape (‘dip’ type). In the second part, the wheelset is going up and the dynamic force becomes negative – the wheel-rail contact upload occurs. After crossing over the isolated error, the wheelset tends to maintain its ascendant course, which leads again to the contact download (the dynamic force will be positive).

**Table 2.** The maximum dynamic forces when crossing over the isolated error.

Damping ratio of the track	$z_t = 0,1$	$z_t = 0,2$	$z_t = 0,3$
Velocity	Dynamic forces [kN]		
$V = 100$ km/h	5.83	5.25	4.84
$V = 200$ km/h	22.54	20.32	18.80

It can observe that for this type of isolated error, the highest dynamic forces become smaller as long as  $z_t$  increases (see Table 2). The maximum values of the dynamic forces in Table 2 help with the analysis of the influence of the velocity at which the wheelset crosses the isolated error. When velocity is double, the dynamic forces will be almost fourfold in value.

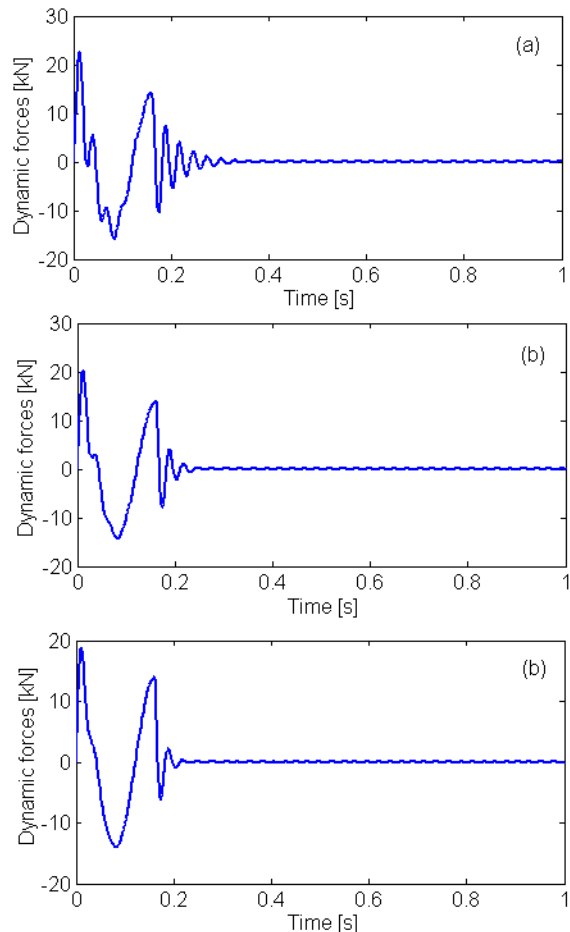


**Fig. 11.** Dynamic forces when crossing over the isolated error at velocity of 200 km/h: (a)  $z_t = 0.1$ ; (b)  $z_t = 0.2$ ; (c)  $z_t = 0.3$ .

**7. Conclusions**

Wheel-rail dynamic forces have to be limited according to homologation criterion which refers to the fatigue stress of the track. The size of such forces mainly depends on the velocity and the characteristics of the track irregularities, which have been underlined in this paper, based on the results from the numerical simulations. Three different situations have been considered to study the magnitude of the wheel-rail dynamic forces when wheel is running over a track with random irregularities, track with joints and track with isolated error, respectively.

When the wheelset is rolling along a track with random irregularities, the frequency-domain analysis shows that the dynamic forces increase with wheelset velocity and reach the highest values at the resonance frequency of the wheel/track system. On the other hand, the influence of the track and of its damping upon the dynamic forces has been proven, while noting that they have the highest values when the wheelset is rolling over a low level quality and low stiffness track.

When the wheelset is running along the track with joints, the dynamic forces increase also as long as either the velocity or the track irregularities amplitude increases. It is about an increase by circa 75% of the dynamic forces when the velocity doubles and by circa 43% when the amplitude of the track geometric irregularities rises by 2 mm.

Upon examining the time-related evolution of the dynamic forces when the wheelset is crossing over an isolated track error, the conclusion is that the dynamic forces can increase by circa 4 times when the velocity doubles.

When the track damping degree is higher, these values can be lowered.

### Acknowledgments

This work has been funded by University Politehnica of Bucharest, through the "Excellence Research Grants" Program, UPB – GEX - 2016. Research project title: Research on developing mechanical and numerical models

for the virtual evaluation of the dynamic performances in the railway vehicles (in Romanian). Contract number: 48/26.09.2016.

This is an Open Access article distributed under the terms of the Creative Commons Attribution Licence



### References

1. T.X. Wu, D.J. Thompson, Vibration analysis of railway track with multiple wheels on the rail, *Journal of Sound and Vibration*, **239**, pp. 69-97 (2001).
2. M. Steenbergen, Modelling of wheels and rail discontinuities in dynamic wheel-rail contact analysis, *Vehicle System Dynamics*, **44** (10), pp. 763-787 (2006).
3. T. X. Wu, D.J. Thompson, A hybrid model for the noise generation due to railway wheel flats, *Journal of Sound and Vibration*, **251**, pp. 115-139 (2002).
4. T. Mazilu, Wheel rail vibrations, (in Romanian), Ed. Matrix Rom, Bucureşti (2008).
5. P. Gullers, L. Andersson, R. Lundén, High-frequency vertical wheel-rail contact forces - Field measurements and influence of track irregularities, *Wear*, **265** (9-10), pp. 1472-1478 (2008).
6. K. Karttunen, E. Kabo, A. Ekberg, The influence of track geometry irregularities on rolling contact fatigue, *Wear*, **314** (1-2), pp. 78-86 (2014).
7. K.H. Oostermeijer, Review on short pitch rail corrugation studies, *Wear*, **265**, pp. 1231-1237 (2008).
8. T. Mazilu, Comfort at the rolling stock, (in Romanian), Ed. Matrix Rom, Bucureşti (2003).
9. D.J. Thompson, Wheel/rail contact noise: development and detailed evaluation of a theoretical model for the generation of wheel and rail vibration due to surface roughness, ORE DT 204 (C 163), Utrecht (1988).
10. UIC 518 Leaflet - 4th edition, Testing and approval of railway vehicles from the point of view of their dynamic behaviour – Safety – Track fatigue – Running behaviour (2009).
11. EN 14363, Railway applications - Testing and Simulation for the acceptance of running characteristics of railway vehicles - Running behaviour and stationary tests (2013).
12. M. Dumitriu, I. Sebeşan, On the wheelset vibration due to the stochastic vertical track irregularities, *Applied Mechanics and Materials*, **809-810**, pp 1037-1042 (2015).
13. I. Sebeşan, Dynamic of the railway vehicles, (in Romanian), Ed. Matrix Rom, Bucureşti (2011).
14. J. Pombo, J. Ambrósio, An alternative method to include track irregularities in railway vehicle dynamic analyses, *Nonlinear Dynamics*, **68** (1-2), pp. 161-176 (2012).
15. S. Mohammadzadeh, M. Sangtarashha, H. Molatefi, A novel method to estimate derailment probability due to track geometric irregularities using reliability techniques and advanced simulation methods, *Archive of Applied Mechanics*, **81**, pp. 1621-1637 (2011).
16. Y.Q. Sun, C. Cole, M. Spiriyagin, Study on track dynamic forces due to rail short-wavelength dip errors using rail vehicle-track dynamics simulations, *Journal of Mechanical Science and Technology*, **27** (3), pp. 629-640 (2013).
17. M.X.D. Li, E.G. Berggren, M. Berg, I. Persson, Assessing track geometry quality based on wavelength spectra and track-vehicle dynamic interaction, *Vehicle System Dynamics*, **46** (Supplement), pp. 261-276 (2008).
18. R.C. Sharma, Parametric analysis of rail vehicle parameters influencing ride behavior, *International Journal of Engineering, Science and Technology*, **3** (8), pp. 54-65 (2011).
19. B. Suarez, J. Felez, J.A. Lozano, P. Rodriguez, Influence of the track quality and of the properties of the wheel-rail rolling contact on vehicle dynamics, *Vehicle System Dynamics*, **51** (2), pp. 301-320 (2013).
20. ORE B 176. Bogies with steered or steering wheelsets, Report No. 1: Specifications and preliminary studies, Vol. 2. Specification for a bogie with improved curving characteristics (1989).
21. M. Dumitriu, I. Sebeşan, Ride quality of railway vehicles, (in Romanian), Ed. Matrix Rom, Bucureşti, (2016).
22. M. Dumitriu, On the dynamic ride forces of the vehicle-track system, *Scientific Bulletin of the "Petru Maior" University of Tîrgu Mureş*, **12** (2), pp. 35-40 (2015).